For student paper competition

OFDM Radar Waveform Design for Sparsity-Based Multi-Target Tracking†

Satyabrata Sen, *Student Member, IEEE* and Arye Nehorai, *Fellow, IEEE*
Department of Electrical and Systems Engineering
Washington University in St. Louis
One Brookings Drive, St. Louis, MO 63130, USA
Email: {ssen3, nehorai}@ese.wustl.edu
Phone: 314-935-7520 Fax: 314-935-7500

***Abstract*—We propose a sparsity-based approach to track multiple targets using an orthogonal frequency division multiplexing (OFDM) radar. The use of an OFDM signal increases the frequency diversity of our system as different scattering centers of a target resonate variably at different frequencies. We observe that in a particular pulse interval the targets lie at a few points on the delay-Doppler plane. Hence, we exploit that inherent sparsity to develop a tracking procedure. The non-zero entries of the sparse vector in our model correspond to the target scattering coefficients at different OFDM subcarriers. Therefore, the sparse vector and associated sparse measurement model exhibit block-sparsity property. We design the spectral weights of the transmitting OFDM waveform to minimize the block-coherence measure of the sparse model. In the tracking filter, we develop a block version of the compressive sampling matching pursuit (CoSaMP) algorithm. We present numerical examples to show the performance of our sparsity-based tracking approach and compare with that of a particle filter (PF). The proposed sparsity-based tracking algorithm takes significantly less computational time and provides equivalent, and sometimes better, tracking performance in comparison with the PF-based tracking.**

I. Introduction

The problem of simultaneous detection and tracking of multiple targets has been one of the most relevant and challenging issues in a wide variety of defense and civilian systems [1], [2]. The situation becomes even more complicated when the tracks of two targets cross. In this work, we look into the multi-target tracking problem from a different perspective. We observe that a multi-target scene is generated by keeping track of the range and velocity (delay and Doppler, respectively) of each target over time. Suppose we discretize the delay-Doppler plane into $N_\tau \times N_\beta$ grid points. Then, if number of targets $M \ll N_\tau N_\beta$, the target scene will be *sparse* in the delay-Doppler plane. This enables us to efficiently track the targets by solving a simple sparse recovery algorithm through a linear program, e.g., l_1-minimization [3] or second-order cone programming (SOCP) [4], or a greedy pursuit, e.g., orthogonal matching pursuit (OMP) [5] or compressive sampling matching pursuit (CoSaMP) [6].

In Section II, we first present a state model describing the dynamic behavior of the targets. Then, we develop a parametric measurement model considering an orthogonal frequency division multiplexing (OFDM) radar [7]. The frequency diversity of OFDM provides additional information as different scattering centers of a target resonate at different frequencies. Next, by exploiting the sparsity in the delay-Doppler plane, we convert the OFDM measurement model to an equivalent sparse measurement model. The non-zero components of the sparse vector, which correspond to the scattering coefficients of the targets at multiple OFDM subcarriers, occur in clusters (blocks). Hence, such vectors are referred to as block-sparse [8], [9].

To minimize the block-coherence measure [10] of the sparse measurement matrix, in Section III, we design the parameters of the transmitting OFDM signal. We prove that the minimum value of block-coherence is attainable when equal amounts of energy are transmitted over the available OFDM subcarriers and that minimum value is inversely proportional to the number of OFDM subcarriers. Hence, this reconfirms the advantage of using OFDM signals. In Section IV, as the sparse recovery algorithm, we propose to exploit the same block-sparsity property by developing a block version of the CoSaMP algorithm, termed BCoSaMP. The simple, iterative greedy structure of the conventional CoSaMP algorithm allows us to easily incorporate the block-sparsity nature of the sparse vector, instead of treating it as a conventional sparse vector and thereby ignoring the additional structure in the problem.

To analyze the performance of our sparsity-based tracking method, in Section V we present numerical examples. At each pulse interval, we dynamically partition a smaller portion of the delay-Doppler plane depending on the predicted state parameters. We compare the resulting tracking performance with that of a particle filter (PF) [11]. Our results show that the sparsity-based tracking algorithm not only takes much less time than that of the PF-based tracking procedure, but also achieves equal (and sometimes better) tracking performance. Finally, concluding remarks and some thoughts on a few unaddressed issues are given in Section VI.

II. Problem Description and Modeling

Fig. 1 presents a schematic representation of the problem scenario. We consider an OFDM radar system that overlooks a region of interest containing multiple moving targets. We

†This work was supported by the Department of Defense under the AFOSR MURI Grant FA9550-05-1-0443 and the ONR Grant N000140810849.

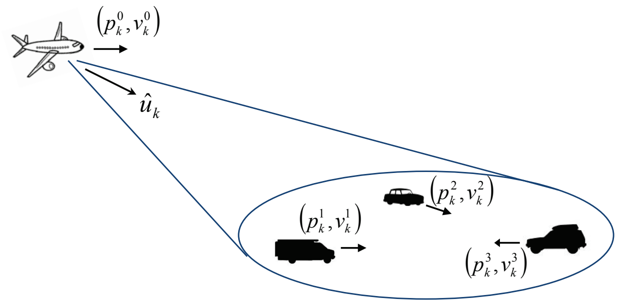

Fig. 1. A schematic representation of multi-target tracking scenario (not drawn to scale).

assume that the targets are at far-field with respect to the radar, and at a particular pulse interval all the targets can be associated with the same direction-of-arrival (DOA) unit vectors $\widehat{\boldsymbol{u}}$.

A. Target Dynamic Model

Suppose there are M targets in the region of interest. Assuming constant velocity movement, we obtain a linear dynamic state equation of the m-th target ($m = 1, 2, \ldots, M$) at the k-th pulse interval as

$$\boldsymbol{x}_k^m = \begin{bmatrix} \boldsymbol{I}_3 & T\boldsymbol{I}_3 \\ \boldsymbol{0} & \boldsymbol{I}_3 \end{bmatrix} \boldsymbol{x}_{k-1}^m + \boldsymbol{w}_k^m, \qquad \text{for } k = 1, 2, \ldots, \tag{1}$$

where $\boldsymbol{x}_k^m \triangleq [\, x_k^m,\, y_k^m,\, z_k^m,\, \dot{x}_k^m,\, \dot{y}_k^m,\, \dot{z}_k^m \,]^T$ and T is the pulse repetition interval (PRI). However, instead of the position and velocity, the radar tracks the targets using their associated delays (τ) and Doppler factors (β). Hence, we can obtain a modified state dynamic model as

$$\bar{\boldsymbol{x}}_k^m = \begin{bmatrix} 1 & T \\ 0 & 1 \end{bmatrix} \bar{\boldsymbol{x}}_{k-1}^m + \begin{bmatrix} T \\ 0 \end{bmatrix} \beta_{k-1}^{\mathrm{r}} + \bar{\boldsymbol{w}}_k^m, \tag{2}$$

where $\bar{\boldsymbol{x}}_k^m \triangleq [\tau_k^m,\, \beta_k^m]^T$, β_{k-1}^{r} denotes the Doppler effect only due to the motion of the radar, and $\bar{\boldsymbol{w}}$ represents the model error.

B. OFDM Measurement Model

We consider an OFDM signalling system with L active subcarriers, a bandwidth of B Hz, and pulse duration of T_{p} seconds. Let $\boldsymbol{a} \triangleq [a_0, a_1, \ldots, a_{L-1}]^T$ represent the complex weights transmitted over the L subcarriers and satisfying $\sum_{l=0}^{L-1} |a_l|^2 = 1$. The subcarrier spacing is denoted as $\Delta f = B/(L+1) = 1/T_{\mathrm{p}}$. Then, the discrete version of the complex envelope of the received signal at the output of the l-th subchannel is given by

$$y_l(t_n) = \sum_{m=1}^{M} a_l\, \zeta_l^m\, \phi_l(t_n, \tau_k^m, \beta_k^m) + e_l(t_n), \qquad \text{for } l = 0, 1, \ldots, L-1,\ n = 0, 1, \ldots, N-1, \tag{3}$$

where

- ζ_l^m is a complex quantity representing the scattering coefficient of the m-th target along the l-th subchannel.
- τ_k^m and β_k^m are the roundtrip delay and Doppler factor of the m-th target, respectively.
- $\phi_l(\cdot)$ is defined as
$$\phi_l(t_n, \tau_k^m, \beta_k^m) \triangleq e^{-j2\pi f_l \tau_k^m}\, e^{j\,2\pi f_l \beta_k^m (t_n - \tau_k^m)}\, I_{[\tau_k^m]}(t_n). \tag{4}$$
- N denotes the number of temporal samples per pulse transmission, covering the range of delays corresponding to a region of interest ($T_{\mathrm{p}} < t_0 < \ldots < t_{N-1} < T$).
- The sampling interval or time resolution $\Delta t \triangleq t_i - t_{i-1}$ depends on the bandwidth of the signal transmitted by the radar, i.e., $\Delta t = 1/(2B) = T_{\mathrm{p}}/\,(2(L+1))$.
- The indicator function $I_{[\tau_k^m]}(t_n)$ is 1 only when $\tau_k^m < t_n < \tau_k^m + T_{\mathrm{p}}$, and 0 otherwise.
- $e_l(t_n)$ represents an aggregation of any static clutter returns and measurement noise at baseband.

From the definition of $I_{[\tau_k^m]}(t_n)$, we find that for each target there will be $N_{\mathrm{s}} \triangleq T_{\mathrm{p}}/\Delta t = 2(L+1)$ temporal samples corresponding to target returns plus clutter and noise. For example, in (3), the m-th target responses will be found at $n = n^m, \ldots, n^m + N_{\mathrm{s}} - 1$, where $n^m = \lceil \tau_k^m/\Delta t \rceil - t_0/\Delta t$. Hence, out of N measurements, at most MN_{s} samples will bear the target responses plus clutter and noise, while the rest correspond to only clutter and noise.

Stacking the measurements of all L subchannels and N temporal points into a vector of dimension $LN \times 1$, we obtain the OFDM measurement model at the k-th pulse interval as

$$\boldsymbol{y}_k = \sum_{m=1}^{M} \overline{\boldsymbol{\Phi}}(\tau_k^m, \beta_k^m)\, \boldsymbol{A}\, \boldsymbol{\zeta}^m + \boldsymbol{e}_k, \tag{5}$$

where

- $\boldsymbol{y}_k = \left[\ldots, \boldsymbol{y}(t_n)^T, \ldots\right]^T$, $\boldsymbol{y}(t_n) = [\ldots, y_l(t_n), \ldots]^T$.
- $\overline{\boldsymbol{\Phi}}(\tau_k^m, \beta_k^m) = \left[\cdots\ \boldsymbol{\Phi}(t_n, \tau_k^m, \beta_k^m)^T\ \cdots\right]^T$ is an $LN \times L$ matrix containing the delay and Doppler information of the m-th target, and $\boldsymbol{\Phi}(t_n, \tau_k^m, \beta_k^m) = \mathrm{diag}\,(\ldots, \phi_l(t_n, \tau_k^m, \beta_k^m), \ldots)$.
- $\boldsymbol{A} = \mathrm{diag}(\boldsymbol{a})$.
- $\boldsymbol{\zeta}^m = [\ldots, \zeta_l^m, \ldots]^T$ is an $L \times 1$ vector having the m-th target scattering coefficients over all subchannels.
- $\boldsymbol{e}_k = \left[\ldots, \boldsymbol{e}(t_n)^T, \ldots\right]^T$ is an $LN \times 1$ vector comprising static clutter, noise, and $\boldsymbol{e}(t_n) = [\ldots, e_l(t_n), \ldots]^T$.

C. Sparse Measurement Model

Sparsity-based signal processing [12]-[14] recently has received significant attentions in many fields. Consider that at the k-th pulse interval we can discretize the possible values of delay and Doppler in N_τ and N_β grid points, respectively, and denote $N_{\mathrm{G}} = N_\tau N_\beta$. Recognizing that each of the M targets can occupy one such delay-Doppler grid point, we can rewrite (5) as

$$\boldsymbol{y}_k = \sum_{i=1}^{N_\tau} \sum_{j=1}^{N_\beta} \overline{\boldsymbol{\Phi}}(\tau_k^i, \beta_k^j)\, \boldsymbol{A}\, \widetilde{\boldsymbol{\zeta}}^{ij} + \boldsymbol{e}_k, \tag{6}$$

where

$$\widetilde{\boldsymbol{\zeta}}^{ij} = \begin{cases} \boldsymbol{\zeta}^m, & \text{if } \tau_k^i = \tau_k^m \quad \text{and} \quad \beta_k^j = \beta_k^m \\ 0, & \text{otherwise} \end{cases}. \tag{7}$$

Therefore, considering all possible combinations of (τ_k^i, β_k^j), $i = 1, \ldots, N_\tau$, $j = 1, \ldots, N_\beta$, we can form an equivalent sparse measurement model as

$$\boldsymbol{y}_k = \widetilde{\boldsymbol{\Phi}}_k \widetilde{\boldsymbol{\zeta}} + \boldsymbol{e}_k, \tag{8}$$

where

- $\widetilde{\boldsymbol{\zeta}}$ is an $LN_\text{G} \times 1$ block-sparse vector, having in total LM non-zero entries, distributed over M blocks with each block is of length L. Hence, the block-sparsity level is equal to the number of targets, i.e., $S = M \ll N_\text{G}$.
- $\widetilde{\boldsymbol{\Phi}}_k = \left[\overline{\boldsymbol{\Phi}}(\tau_k^1, \beta_k^1)\boldsymbol{A} \;\cdots\; \overline{\boldsymbol{\Phi}}(\tau_k^{N_\tau}, \beta_k^{N_\beta})\boldsymbol{A}\right]$ is an $LN \times LN_\text{G}$ block-sparse measurement matrix, where each block of columns, $\overline{\boldsymbol{\Phi}}(\tau_k^i, \beta_k^j)\boldsymbol{A}$, is of dimension $LN \times L$.

III. OFDM Waveform Design

The block-coherence measure, μ, of the block-sparse system matrix, $\widetilde{\boldsymbol{\Phi}}_k$, in (8) plays a similar role as the coherence of the conventional sparse measurement matrix. Therefore, to maximize accuracy in the sparse-recovery, it is desirable to have its value as small as possible. To compute the expression of μ, we consider two separate blocks of columns of the measurement matrix (i.e., either $i \neq i'$ or $j \neq j'$, when $i, i' = 1, \ldots, N_\tau,\; j, j' = 1, \ldots, N_\beta$), and get

$$\left[\overline{\boldsymbol{\Phi}}(\tau_k^i, \beta_k^j)\boldsymbol{A}\right]^H \left[\overline{\boldsymbol{\Phi}}(\tau_k^{i'}, \beta_k^{j'})\boldsymbol{A}\right] = \boldsymbol{A}^H \boldsymbol{Q} \boldsymbol{A}, \tag{9}$$

where $\boldsymbol{Q}$ is an $L \times L$ diagonal matrix, expressed as

$$\boldsymbol{Q} = \text{diag}\left(\ldots, \xi(l)\, e^{j\,2\pi\,\zeta(l)}, \ldots\right), \quad l = 0, \ldots, L-1, \tag{10}$$

and

$$\begin{aligned} \xi(l) &= \widetilde{N}\, \text{sinc}\left(\widetilde{N}\, f_l\, (\beta_k^j - \beta_k^{j'})\, \Delta t\right), \\ &\approx \widetilde{N} \;=\; N_\text{s} - \left(n^{i'} - n^i\right), \\ \zeta(l) &= f_l \left[(1 + \beta_k^j)\, \tau_k^i - (1 + \beta_k^{j'})\, \tau_k^{i'} \right. \\ &\qquad \left. -(\beta_k^j - \beta_k^{j'})\,(t_{n^{i'}} + t_{n^i + N_\text{s} - 1})/2\right], \end{aligned}$$

with $n^i = \lceil \tau_k^i / \Delta t \rceil - t_0/\Delta t$ and $n^{i'} = \lceil \tau_k^{i'} / \Delta t \rceil - t_0/\Delta t$. Therefore, from the definitions of $\boldsymbol{A}$ and $\boldsymbol{Q}$, it follows that $\boldsymbol{A}^H \boldsymbol{Q} \boldsymbol{A}$ is also an $L \times L$ diagonal matrix whose eigenvalues are equal to the entries on the main diagonal, i.e.,

$$\lambda_l(\boldsymbol{A}^H \boldsymbol{Q} \boldsymbol{A}) = |a_l|^2\; \xi(l)\, e^{j\,2\pi\,\zeta(l)}, \quad \text{for } l = 0, \ldots, L-1, \tag{11}$$

and hence the corresponding spectral radius is

$$\begin{aligned} \rho(\boldsymbol{A}^H \boldsymbol{Q} \boldsymbol{A}) &= \max_l |a_l|^2\, |\xi(l)|\,, \\ &\approx \left[N_\text{s} - \left(n^{i'} - n^i\right)\right] \max_l |a_l|^2\,, \\ &= \left[2(L+1) - \left(n^{i'} - n^i\right)\right] \max_l |a_l|^2. \end{aligned} \tag{12}$$

Therefore, the block-coherence of $\widetilde{\boldsymbol{\Phi}}_k$ is expressed as [10]

$$\begin{aligned} \mu &= \max_{\substack{(i,j),(i',j'):\\ i \neq i' \text{ or } j \neq j'}} \frac{1}{L}\left[2(L+1) - \left(n^{i'} - n^i\right)\right] \max_l |a_l|^2\,, \\ &= \frac{2(L+1)}{L} \max_l |a_l|^2\,, \quad \text{when } i = i' \text{ but } j \neq j'. \end{aligned} \tag{13}$$

To minimize the value of μ, we have to minimize the effect of $\max_l\, |a_l|^2$ in the numerator of (13). The minimum value of μ can be achieved when we transmit equal amounts of energy over all the OFDM subcarriers, i.e., $|a_l|^2 = 1/L$, $\forall\, l$. This is the consequence of the following theorem.

Theorem 1. *Given L complex coefficients $\{a_0, a_1, \ldots, a_{L-1}\}$ such that $\sum_{l=0}^{L-1} |a_l|^2 = 1$,*

$$\min_{\{a_0, \ldots, a_{L-1}\}} \max_l |a_l|^2 = \frac{1}{L}\,,$$

and it is achievable when $|a_l|^2 = 1/L\; \forall\, l$.

Proof: Contrary to the statement of the theorem, assume that it is possible to select a_l's in such a way that $\max_l\, |a_l|^2 < 1/L$. However, from the constraint equation $\sum_{l=0}^{L-1} |a_l|^2 = 1$ we note that if $|a_l|^2 < 1/L$ is satisfied for any l, then there would exist at least another l' for which $|a_{l'}|^2 > 1/L$, and therefore $\max_l\, |a_l|^2 < 1/L$ would not be satisfied. Hence, the minimum value of $\max_l |a_l|^2$ could be only $1/L$ and that could be achieved when $|a_l|^2 = 1/L\; \forall\, l$. ■

Therefore, considering one of the simplest choices with $a_l = 1/\sqrt{L}\; \forall\, l$, we can write a modified version of (8) as

$$\boldsymbol{y}_k = \widetilde{\widetilde{\boldsymbol{\Phi}}}_k\, \widetilde{\boldsymbol{\zeta}} + \boldsymbol{e}_k, \tag{14}$$

where $\widetilde{\widetilde{\boldsymbol{\Phi}}}_k = (1/\sqrt{L})\, \left[\overline{\boldsymbol{\Phi}}(\tau_k^1, \beta_k^1)\; \cdots \overline{\boldsymbol{\Phi}}(\tau_k^{N_\tau}, \beta_k^{N_\beta})\right]$. Consequently, the block-coherence of $\widetilde{\widetilde{\boldsymbol{\Phi}}}_k$ becomes $\widetilde{\mu} = 2(L+1)/L^2$.

Note that $\widetilde{\mu} = 2(L+1)/L^2$ implies that it would be advantageous to increase the value of L (i.e., the number of OFDM subcarriers) as much as possible. However, given a fixed bandwidth of operation, as we increase the value of L, the subcarrier spacing Δf decreases, i.e., two adjacent subcarriers come closer to each other on the frequency axis. Then, it may happen that the variations of the target responses become insignificant over the adjacent subcarriers, and hence we do not achieve any improvement. Therefore, the value of L is to be chosen as a compromise between the expected variability of the target responses over different frequencies and the block-coherence measure of the measurement matrix.

IV. Tracking Filter

Any tracking procedure is a sequential method consisting of repeated applications of two sub-procedures: prediction and update. In the prediction stage, the previous estimated state $(\bar{\boldsymbol{x}}_{k-1})^+$ is substituted into the state dynamic equation (2) to obtain a predicted state $(\bar{\boldsymbol{x}}_k)^-$ at the k-th pulse interval. Then, in the update stage, the new measurement $\boldsymbol{y}_k$ from (5) is used to modify the predicted state $(\bar{\boldsymbol{x}}_k)^-$ and obtain the estimated state $(\bar{\boldsymbol{x}}_k)^+$ at the k-th pulse interval.

To exploit the inherent sparsity on the delay-Doppler plane, we employ a block version of the conventional CoSaMP recovery algorithm, called block-CoSaMP or BCoSaMP, in the update stage. Our approach stems from [15, Algo. 1]. From the discussion of the previous section, we notice that the sparse vector in our model shows a block structure, which is important to incorporate in the recovery algorithm. The simple and iterative greedy structure of the conventional CoSaMP algorithm helps us to easily integrate this block-sparsity nature of the sparse vector into our algorithm.

V. Numerical Results

We present numerical examples to demonstrate the performance of our proposed sparsity-based tracking approach. Fig. 1 schematically describes a scenario that we used in the simulations. The radar was at height $z = 1$ km above the ground and moving with a velocity $33.33\,(= 33.33\,\hat{j})$ m/s, which is approximately 120 kph. We considered that it is looking over an area that spans a range of roundtrip delays (t_0, t_{N-1}) with $N = 120$ and has center at $(x, y) = (3, 2)$ km. There were two moving targets within the region of interest. The first target started at a position $(x, y, z) = (3000, 2000, 0)$ m and was moving with a velocity of $16.67\,(= 16.67\,\cos(5°)\,\hat{i} + 16.67\,\sin(5°)\,\hat{j})$ m/s, which is approximately 60 kph. The scattering parameters of this target was assumed to be the same for all subchannels, i.e., $\boldsymbol{\zeta}^1 = [1, 1, 1, 1]^T$. The second target started at a position $(x, y, z) = (3010, 2006, 0)$ m and was moving with a velocity of $12.5\,(= 12.5\,\cos(-5°)\,\hat{i} + 12.5\,\sin(-5°)\,\hat{j})$ m/s, which is approximately 45 kph. The scattering parameters of the second target was assumed to be quite different across the subchannels, i.e., $\boldsymbol{\zeta}^2 = [0.01, 0.5, 1.1, 1.6]^T$. We considered the radar parameters as: carrier frequency $f_c = 1$ GHz; bandwidth $B = 100$ MHz; number of OFDM subcarriers $L = 4$; subcarrier spacing $\Delta f = B/(L+1) = 20$ MHz; pulse width $T_p = 1/\Delta f = 50$ ns; pulse repetition interval $T = 10$ ms; transmitted OFDM weights were the same, i.e., $a_l = 1/\sqrt{L}\ \forall l$.

We used the BCoSaMP algorithm to track the targets. We considered regular (uniform) grids to partition the delay-Doppler plane having a delay resolution of $\Delta\tau = 3.33$ ns (i.e., corresponding to a range resolution of 0.5 m) and a Doppler resolution of $\Delta\beta = 2.46 \times 10^{-9}$ (i.e., corresponding to a velocity resolution of 1 m/s). We dynamically partitioned a small portion of the delay-Doppler plane at a particular pulse interval, instead of using all the possible delay-Doppler grids for every pulse interval. This could be done because at every pulse interval the predicted state provides a rough approximation of the new estimated state. Therefore, we first used (2) to compute the predicted values of delay, $(\tau_k^m)^-$, and Doppler, $(\beta_k^m)^-$, for both the targets at the k-th pulse interval. Then, to form grids we selected a small region of the delay-Doppler plane as

$$\mathcal{R} \;:=\; \bigcup_{i=1,2} \left[(\tau_k^i)^- - \bar{\tau}/2, (\tau_k^i)^- + \bar{\tau}/2\right] \times \left[(\beta_k^i)^- - \bar{\beta}/2, (\beta_k^i)^- + \bar{\beta}/2\right], \quad (15)$$

where $\bar{\tau}$ and $\bar{\beta}$ define the total area around $((\tau_k^i)^-, (\beta_k^i)^-)$ in which we expect to get the state estimates at the k-th pulse. In our simulations, we chose $\bar{\tau} = 40\Delta\tau$ and $\bar{\beta} = 4\Delta\beta$.

We compared the resultant tracking performance with that of a particle filter (PF). We augmented the state vector with the scattering coefficients of the targets along with their positions and velocities. The temporal evaluation of the scattering coefficients was assumed to be constant, i.e., $\boldsymbol{\zeta}^m(k) = \boldsymbol{\zeta}^m(k-1),\ m = 1, 2$. This assumption is in general true when the target is far away from the radar, as in our case. Both the state and measurement noise processes were assumed to be zero-mean Gaussian processes. We generated the state particles from an importance density function, which we chose to be the transitional prior $p\left(\boldsymbol{x}_k^{(i)} | \boldsymbol{x}_{k-1}^{(i)}\right),\ i = 1, 2, \ldots, N_x$, where N_x is the number of state particles. In our simulations, we considered $N_x = 800$ state particles. The importance weights were realized as $w_k^{(i)} \propto w_{k-1}^{(i)} p\left(\boldsymbol{y}_k | \boldsymbol{x}_k^{(i)}\right)$.

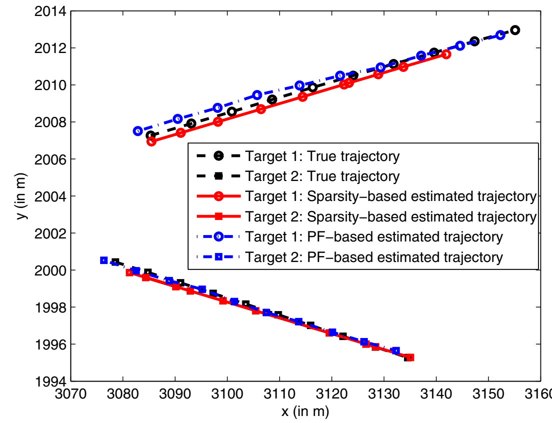

(a)

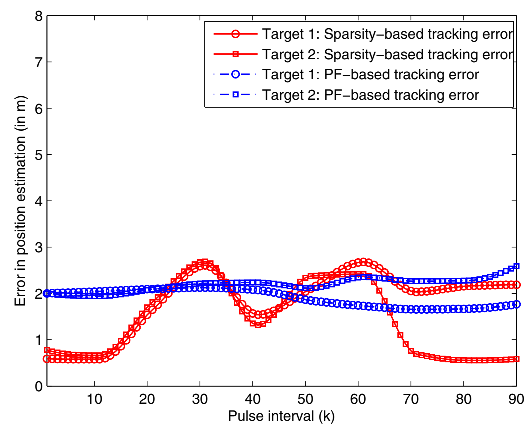

(b)

Fig. 2. Comparison of (a) the true and estimated trajectories and (b) associated root-mean-squared errors in position estimation of two non-crossing target paths using the sparsity-based and PF-based tracking algorithms.

Figs. 2 and 3 depict the tracking performance and associated errors in position estimation for two non-crossing and crossing target paths, respectively. It is evident from these plots that, compared to the PF-based approach, the sparsity-based tracking approach provides equivalent tracking performances, and sometimes even better when the target paths are not crossing. In addition, our sparsity-based approach provided estimation results much quicker than that of PF-based algorithm. We

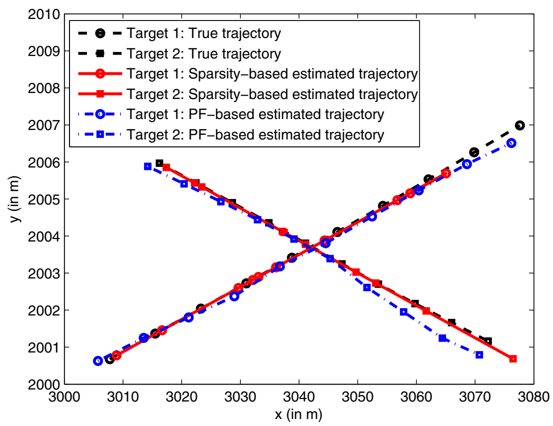

(a)

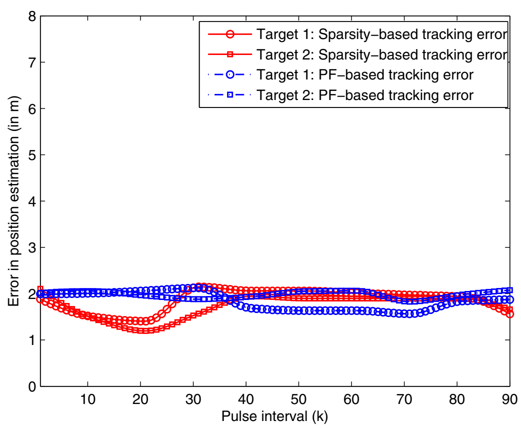

(b)

Fig. 3. Comparison of (a) the true and estimated trajectories and (b) associated root-mean-squared errors in position estimation of two crossing target paths using the sparsity-based and PF-based tracking algorithms.

found that on average the PF-based approach took 131.25 s to estimate the target state per pulse interval; whereas sparsity-based technique took only 17.87 s (for non-crossing target paths) and 6.85 s (for crossing target paths), which is one order less than that of the PF-based tracking. The difference in times in the sparsity-based approach, corresponding to the non-crossing and crossing target paths, occurs due to the dynamic computation of the delay-Doppler grids over region $\mathcal{R}$, as specified in (15). When the target paths cross each other the size of $\mathcal{R}$ is smaller, and hence it takes lesser time to calculate the grid values.

VI. Conclusions

In this paper, we addressed the problem of tracking multiple targets in a region of interest. Observing that the target scene is sparse on the delay-Doppler plane, we proposed a sparsity-based tracking approach. First, we presented a dynamic state model, and then a parametric measurement model of an orthogonal frequency division multiplexing (OFDM) radar. The use of an OFDM signal increased the frequency diversity of our system, as different scattering centers of a target resonate variably at different frequencies. Then, by exploiting the sparsity in the delay-Doppler plane, we formulated an equivalent block-sparse measurement model, in which the non-zero components of the sparse vector correspond to the scattering coefficients of the targets at different OFDM subcarriers. In addition, we designed the spectral weights of the transmitting OFDM waveform for the minimum block-coherence measure, and proved that is attainable by transmitting equal amounts of energy over all the subcarriers. In the tracking filter, we used a block version of the compressive sampling matching pursuit (CoSaMP) algorithm. We presented numerical examples to show the performance of our sparsity-based tracking approach and compared it with the performance of a particle filter (PF) based tracking procedure. The sparsity-based tracking algorithm took much less time and provided equivalent tracking performance in comparison to the PF-based tracking. In our future work, we will study the effects of compressive sensing (CS) by pre-multiply the measurement vector with a random matrix. We will also validate the performance of our proposed tracker with real data.

References

[1] S. S. Blackman, *Multiple-Target Tracking with Radar Applications*. Dedham, MA: Artech House, Inc., Dec. 1986.

[2] Y. Bar-Shalom, *Multitarget-Multisensor Tracking: Advanced Applications*. Boston, MA: Artech House, Inc., 1990.

[3] S. S. Chen, D. L. Donoho, and M. A. Saunders, "Atomic decomposition by basis pursuit," *SIAM Jour. on Scientific Computing*, vol. 20, no. 1, pp. 33–61, Aug. 1998.

[4] D. Malioutov, M. Çetin, and A. S. Willsky, "A sparse signal reconstruction perspective for source localization with sensor arrays," *IEEE Trans. Signal Process.*, vol. 53, no. 8, pp. 3010–3022, Aug. 2005.

[5] S. G. Mallat and Z. Zhang, "Matching pursuits with time-frequency dictionaries," *IEEE Trans. Signal Process.*, vol. 41, no. 12, pp. 3397–3415, Dec. 1993.

[6] D. Needell and J. Tropp, "CoSaMP: Iterative signal recovery from incomplete and inaccurate samples," *Applied and Computational Harmonic Analysis*, vol. 26, no. 3, pp. 301–321, May 2009.

[7] A. Pandharipande, "Principles of OFDM," *IEEE Potentials*, vol. 21, no. 2, pp. 16–19, Apr. 2002.

[8] Y. C. Eldar and M. Mishali, "Robust recovery of signals from a structured union of subspaces," *IEEE Trans. Inf. Theory*, vol. 55, no. 11, pp. 5302–5316, Nov. 2009.

[9] Y. C. Eldar and H. Bölcskei, "Block-sparsity: Coherence and efficient recovery," in *IEEE Int. Conf. on Acoustics, Speech, and Signal Proc.*, Taipei, Taiwan, Apr. 19–24, 2009, pp. 2885–2888.

[10] Y. Eldar, P. Kuppinger, and H. Bölcskei, "Block-sparse signals: Uncertainty relations and efficient recovery," *IEEE Trans. Signal Process.*, vol. 58, no. 6, pp. 3042–3054, Jun. 2010.

[11] B. Ristic, S. Arulampalam, and N. Gordon, *Beyond the Kalman Filter: Particle Filters for Tracking Applications*. Boston, MA: Artech House Publishers, Feb. 2004.

[12] E. J. Candès, J. Romberg, and T. Tao, "Robust uncertainty principles: Exact signal reconstruction from highly incomplete frequency information," *IEEE Trans. Inf. Theory*, vol. 52, no. 2, pp. 489–509, Feb. 2006.

[13] D. L. Donoho, "Compressed sensing," *IEEE Trans. Inf. Theory*, vol. 52, no. 4, pp. 1289–1306, Apr. 2006.

[14] E. Candès and M. Wakin, "An introduction to compressive sampling [A sensing/sampling paradigm that goes against the common knowledge in data acquisition]," *IEEE Signal Process. Mag.*, vol. 25, no. 2, pp. 21–30, Mar. 2008.

[15] R. G. Baraniuk, V. Cevher, M. F. Duarte, and C. Hegde, "Model-based compressive sensing," *IEEE Trans. Inf. Theory*, vol. 56, no. 4, pp. 1982–2001, april 2010.